Modeling of Assembled Combustion Engine Parts under Consideration of Micro Slip Effects in the Connection Flanges

C. Schedlinski [1), **A. Genzo** [2), **B. Läer** [2), **L. Panning** [3)

[1) ICS Engineering GmbH
    D-63225 Langen, Germany
    email: **sched@ics-engineering.com**

[2) Volkswagen AG
    D-38436 Wolfsburg, Germany

[3) Universität Hannover
    Institut für Dynamik und Schwingungen
    D-30167 Hannover, Germany

Abstract

This paper addresses the modeling of assembled combustion engine parts. Here multiple flange connections are found that contribute to the stiffness and damping characteristics. By example of a four cylinder combustion engine a finite element modeling technique will be introduced which focuses on a suitable and proper representation of the flange regions between crankcase and crankshaft main bearing cap. Especially, a numerical method will be presented and applied that accounts for the nonlinear damping and stiffness characteristics of the system. The numerical analysis results will be compared to experimental data in order to prove the effectiveness of the method.

1   Introduction

Combustion engine assemblies comprise multiple flange connections that contribute to the stiffness and damping characteristics of the assembled engine parts and thus influence the dynamic behavior of the system. The underlying phenomena in the flange region must be well understood, and appropriate modeling techniques must be readily available in order to allow for the numerical simulation of the forced vibrations of the system.

By example of a four cylinder combustion engine a finite element (FE) modeling technique will be introduced which focuses on a suitable and proper representation of the flange regions between crankcase and crankshaft main bearing cap. The presented modeling technique enables the determination of the displacements in the flange connection interfaces by means of a modal description. Since the quality of the modal description strongly depends on highly accurate FE models of the individual constitutive engine parts, experimental modal analysis and computational model updating will be applied to obtain sufficient fidelity.

The assembled engine parts are subjected to harmonic external excitation, leading to small relative displacements between the crankcase and the main bearing cap of the engine. These displacements as well as the surface roughness and the varying normal pressure distribution over the flange connection interfaces induce micro slip effects that result in nonlinear damping and stiffness characteristics of the assembly.

Especially, a numerical method will be presented that accounts for the nonlinear damping and stiffness characteristics of the system. Since the method is based on a harmonic balance approach, it provides a harmonic linearization of the nonlinear contact and friction forces emerging from the flange connection.

The linearized contact and friction forces along with the modal description of the single engine parts are used to compute the forced response of the free/free assembly.

The numerical analysis results will be compared to experimental data in order to prove the effectiveness of the method. For the acquisition of the corresponding experimental forced response data of the assembly, a stepped sine measurement technique will be applied with closed-loop control of the excitation force satisfying the assumptions of the underlying harmonic balance approach.

2 Theory

2.1 Modal description of the assembled engine parts

The elastic engine parts, the crankcase and the crankshaft main bearing cap, are discretized using the FE method. The FE models are subjected to a modal reduction to generate a modal description of the linear elastic engine parts. The modal description consists of the natural frequencies $\omega_{0\,j,k}$ and the free vibration mode shapes $\hat{\mathbf{u}}_{j,k}$ determined with a FE analysis as well as the damping values $D_{j,k}$ extracted from an experimental modal analysis with the indices j and k denoting the mode shape number and the engine part, respectively, with $k=1$ indicating the crankcase and $k=2$ the main bearing cap. Assuming that the excitation forces are harmonic with the angular excitation frequency Ω, the system response will be harmonic as well, if linear elastic behavior is assumed. Because of simplicity, in the following the complex notation is used to describe the forces and displacements. Hence, the excitation forces read

$$\mathbf{f}_E(t) = \hat{\mathbf{f}}_E\, e^{i\,\Omega t}\,, \tag{1}$$

the modal coordinates are given by

$$\mathbf{q}(t) = \hat{\mathbf{q}}\; e^{i\,\Omega t} \tag{2}$$

and the physical displacements by

$$\mathbf{w}(t) = \hat{\mathbf{w}}\; e^{i\,\Omega t}\,. \tag{3}$$

The dynamic stiffness matrix $\hat{\mathbf{A}}_k$ containing the modal description of one elastic body (mode shapes normalized to unit modal mass) is defined by

$$\hat{\mathbf{A}}_k = \mathbf{diag}\left(\omega_{0\,j}^2 - \Omega^2 + i\,2\,\omega_{0\,j}\,\Omega\,D_j\right)_k\,. \tag{4}$$

To compose the assembly consisting of the crankcase coupled with the main bearing cap, the modal descriptions of the two bodies are assembled in the dynamic stiffness matrix of the system

$$\hat{\mathbf{A}} = \mathbf{diag}\left(\hat{\mathbf{A}}_k\right) \tag{5}$$

and the vectors containing the modal coordinates and the excitation forces are assembled as well

$$\hat{\mathbf{q}} = \begin{bmatrix} \hat{\mathbf{q}}_1 \\ \hat{\mathbf{q}}_2 \end{bmatrix},\; \hat{\mathbf{f}}_E = \begin{bmatrix} \hat{\mathbf{f}}_{E1} \\ \hat{\mathbf{f}}_{E2} \end{bmatrix}\,. \tag{6}$$

Now, the $j = 1,\dots,N$ free vibration mode shapes describing the deformation of the crankcase and the main bearing cap have to be arranged in the modal transformation matrix $\mathbf{X}$ of the assembly

$$\mathbf{X} = \left(\hat{\mathbf{u}}_{1,1},\dots,\hat{\mathbf{u}}_{N,1},\hat{\mathbf{u}}_{1,2},\dots,\hat{\mathbf{u}}_{N,2}\right)\,. \tag{7}$$

Finally, a contact force vector $\hat{\mathbf{f}}_C$ is introduced to account for the structural couplings between the crankcase and the main bearing cap leading to an equation determining the vibration response of the assembly in the frequency domain in terms of modal (or generalized) coordinates

$$\hat{\mathbf{A}}\,\hat{\mathbf{q}} = \mathbf{X}_E^T\,\hat{\mathbf{f}}_E + \mathbf{X}_C^T\,\hat{\mathbf{f}}_C\,. \tag{8}$$

2.2 Modeling of the flank contacts and flange connections

The coupling of the crankcase and the main bearing cap consists of four interfaces, two bolt connections and two flank contacts (the side flanks of the crankshaft main bearing cap are assembled with oversize leading to compression between crankshaft main bearing cap and crank case) as shown in figure 1.
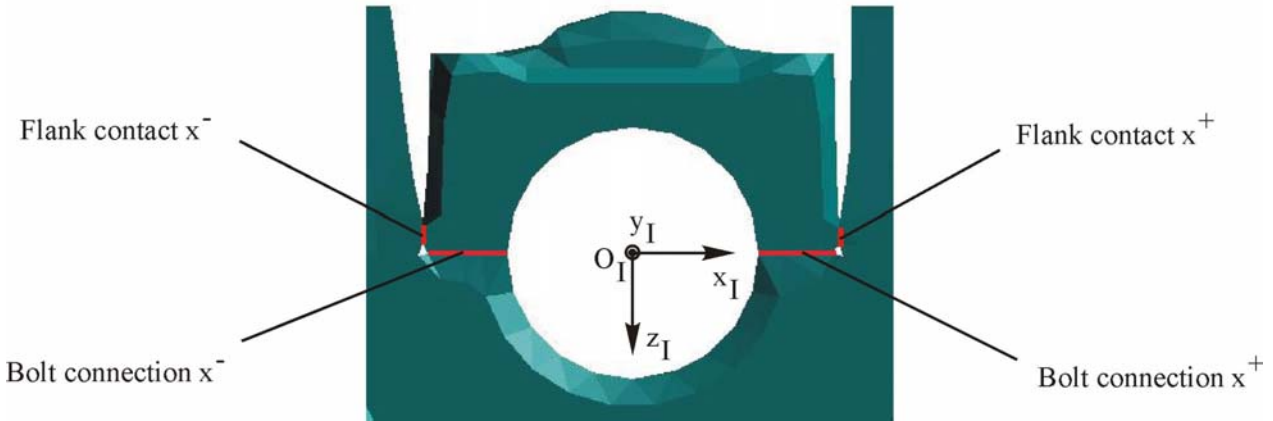

Figure 1: Bolt connections and flank contacts between the crankcase and the main bearing cap

The contact interfaces between the engine parts can be described as surfaces where two bodies get in contact. For the modeling of the contact behavior, the contact surfaces are discretized with contact elements and contact nodes, and at the center of the contact surfaces control points K_i are defined containing the information of the global motion of the contact surfaces in terms of generalized coordinates. Assuming that the elastic deformations in the contact surfaces are small, the motion of the discrete contact nodes can be approximated by the motion of the control points applying rigid body kinematics.

To analyze the relative motion between contact nodes lying at the same position on opposite contact surfaces in the crankcase-main bearing cap assembly, a *point contact model* is used which is described in detail in [3] and [4]. The surface roughness is included in the point contact model by means of the cumulative height distribution with respect of the height of the asperities as described in [5], and is known as the *Abbott curve*. The cumulative height distribution can be interpreted as the percentage contact area when two rough surfaces are pressed together with an average contact normal force F_N. A measurement of a rough surface profile and the corresponding Abbott curve are shown in figures 2a and 2b, respectively. The percentage contact area like that presented in figure 2b can be approximated analytically by a third-order polynomial. The integral of this polynomial can be considered as a description for the nonlinear force-displacement relation in the normal contact direction between opposite contact nodes and accounts for a non-constant normal pressure distribution in the contact surfaces.

Depending on the relative displacements occurring between opposite contact nodes in the normal and tangential directions, micro-slip effects due to the following mechanisms can be modeled in the contact surfaces:

1. The contact elements within one contact surface experience different relative displacement amplitudes and, consequently, while some contact elements slide, others subjected to smaller relative displacements still stick.

2. A non-constant pressure distribution in the contact surface due to surface roughness leads to different contact normal forces for the contact elements which will cause different slip loads, and, thus, slipping and sticking zones exist in one contact surface.
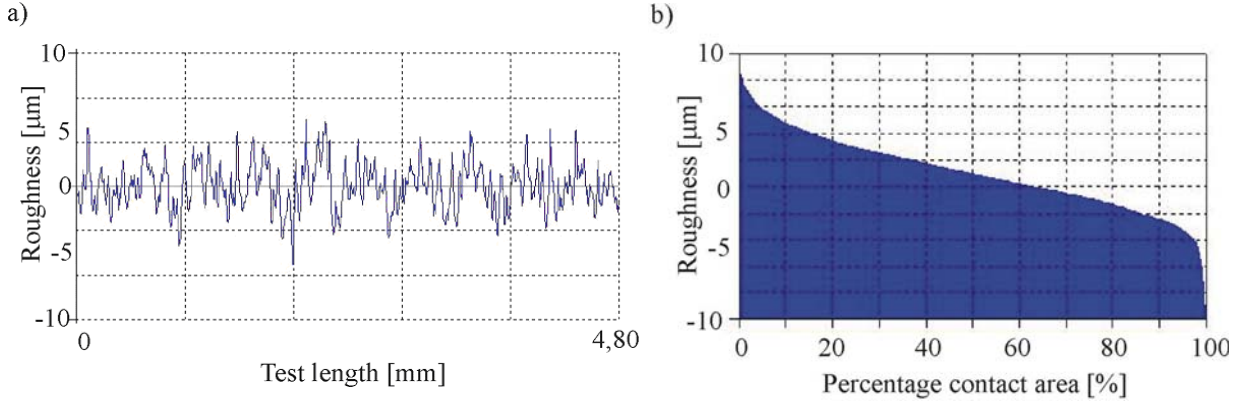
Figure 2: Roughness of surfaces: a) measured surface profile; b) percentage contact area of a)

Note that micro-slip effects represent the main damping mechanism for the flank contacts and the connection flanges of the crankcase-main bearing cap assembly.

The relative displacements $\hat{\mathbf{w}}_C$ in the connection flanges and the flank contacts are determined in terms of the generalized coordinates

$$\hat{\mathbf{w}}_C = -\mathbf{X}_C\,\hat{\mathbf{q}} = -\mathbf{R}_{CI}\,\mathbf{X}\,\hat{\mathbf{q}}, \tag{9}$$

with the modal matrix $\mathbf{X}$ defined in equation (7) and the Matrix $\mathbf{R}_{CI}$ transforming the displacements from the global coordinate system $\left[O_I;\,x_I;\,y_I;\,z_I\right]$ to the coordinate systems $\left[O_C;\,x_C;\,y_C;\,z_C\right]$ attached to the control points in the contact surfaces of the flank contacts and connection flanges, respectively. The contact and friction forces in the contact surfaces are nonlinearly dependent on the relative displacements and on the contact parameters of the point contact model: the global normal contact stiffness c_N, the global tangential contact stiffness c_T, the average contact normal force F_N, the average surface roughness R_Z and the friction coefficient μ.

2.3 Frequency response of the assembled engine parts

Applying the harmonic balance method, the nonlinear force/displacement relations in normal and tangential directions of the contact surfaces are linearized harmonically yielding complex contact stiffness and damping coefficients. These stiffness and damping coefficients are assembled in the complex stiffness matrix $\hat{\mathbf{K}}_C$ and together with equation (9) a description of the harmonically linearized contact and friction forces is obtained

$$\hat{\mathbf{f}}_C = \hat{\mathbf{K}}_C\,\hat{\mathbf{w}}_C = -\hat{\mathbf{K}}_C\,\mathbf{R}_{CI}\,\mathbf{X}\,\hat{\mathbf{q}}. \tag{10}$$

Keeping in mind that $\mathbf{X}_C^T = \mathbf{X}^T\,\mathbf{R}_{CI}^T$ and inserting equation (10) in equation (8) results in the relation

$$\left[\hat{\mathbf{A}} + \mathbf{X}^T\,\mathbf{R}_{CI}^T\,\hat{\mathbf{K}}_C\,\mathbf{R}_{CI}\,\mathbf{X}\right]\hat{\mathbf{q}} = \mathbf{X}_E^T\,\hat{\mathbf{f}}_E. \tag{11}$$

Solving equation (11) iteratively with a damped Newton method, the forced frequency response of arbitrary points lying on the crankcase-main bearing cap assembly can be determined.

3 Example

3.1 Component Model Validation

Initial FE models were available for crank case (figure 3) and crankshaft main bearing cap (figure 4). These models were utilized for test planning at first.
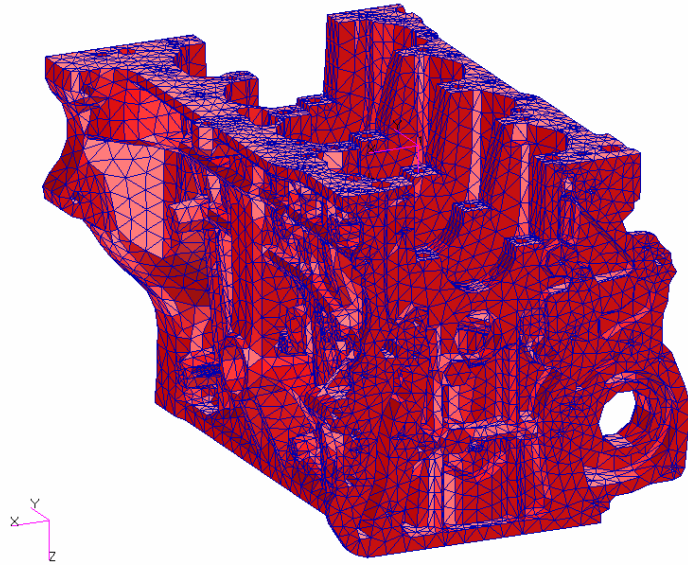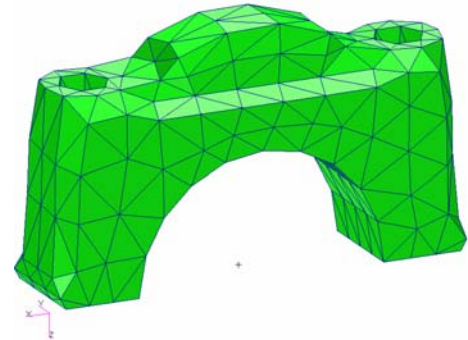
Figure 3: Solid model of crank case

Figure 4: Solid model of crankshaft main bearing cap

Then roving hammer modal tests with multiple references were performed under free/free boundary conditions (bungee cords), and modal parameters were identified subsequently. For the crank case 23 mode shapes could be identified in the investigated frequency range up to 4 kHz, and for the crankshaft main bearing cap three mode shapes were obtained up to 8 kHz. The quality of the identified data was very good.

For the crank case and the crankshaft main bearing cap the correlation before and after validation are shown in tables 1 and 2. For the crank case the model mass was adjusted to the weighed mass of the test item, and the Young's modulus was modified utilizing computational model updating techniques. For the crankshaft main bearing cap only the model mass was adjusted. All in one the initial correlations are already very satisfactory (high MAC values, small frequency deviations). The validation could therefore – in this case – only fine tune the results.

State	Number of Test Modes Available	Number of Test Modes Paired	Mean Frequency Deviation [Hz]	Maximum Frequency Deviation [Hz]	Mean MAC Value [%]	Minimal MAC Value [%]
Initial	23	23	1.74	3.07	94.18	72.72
Validated	23	23	-0.26	-2.72	93.95	70.91

Table 1: Correlation results for crank case

State	Number of Test Modes Available	Number of Test Modes Paired	Mean Frequency Deviation [Hz]	Maximum Frequency Deviation [Hz]	Mean MAC Value [%]	Minimal MAC Value [%]
Initial	3	3	-4.13	-5.68	97.47	95.33
Validated	3	3	-2.95	-4.49	97.48	95.35

Table 2: Correlation results for crankshaft main bearing cap

3.2   Interfaces

For the interfaces of the crankshaft main bearing cap to the crank case, the model shown in figure 5 was applied. The connection was modeled via rigid elements coupling the individual nodes of the joint faces. The bolts were modeled as beams while the nominal diameter of the bolts was applied. The bolts were then as well connected via rigid elements. The flank contacts were not explicitly modeled at this stage.
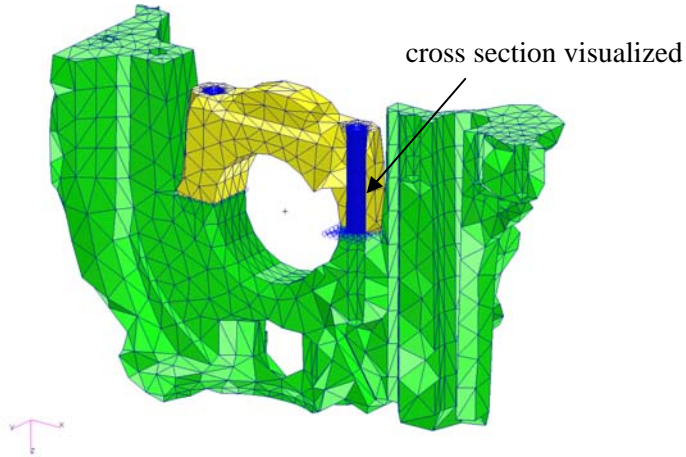

Figure 5: Initial model of bolted interface

After test planning, a roving hammer modal test with multiple references was performed under free/free boundary conditions (bungee cords), and modal parameters were identified subsequently. For the assembly 27 mode shapes could be identified in the investigated frequency range up to 4 kHz. The quality of the identified data was very good except for a small frequency band around 1500 Hz. Here, tilting of the crankshaft main bearing cap occurs.
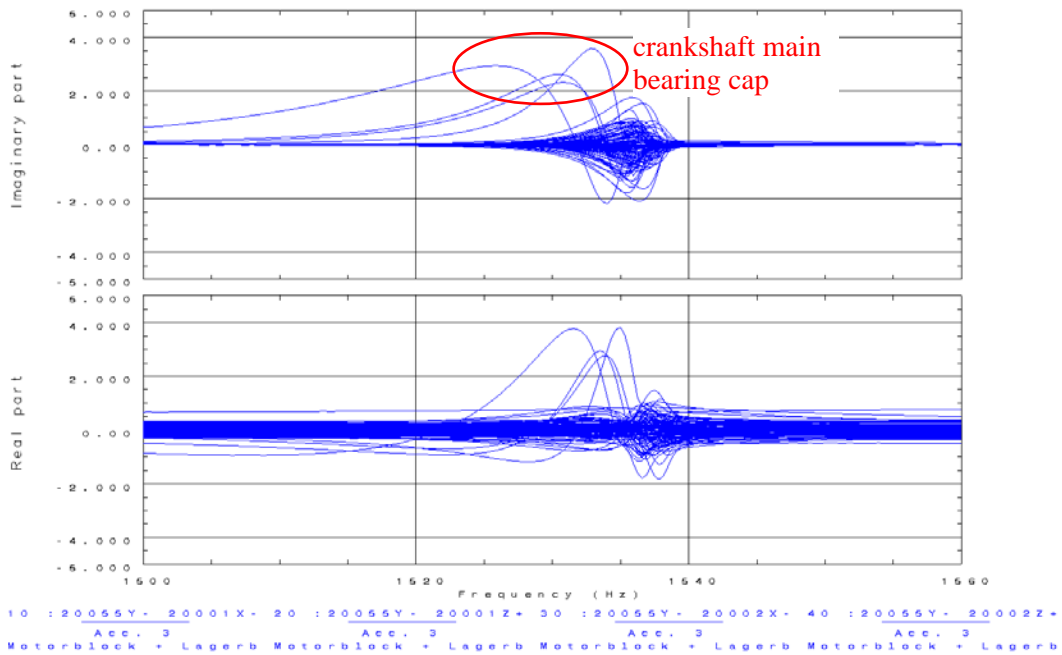

Figure 6: Detail of measured frequency responses for assembly

Figure 6 above shows a detail of the measured frequency responses (all measured degrees of freedom) in the disturbed frequency range for one of the references. Here, clear nonlinear effects can be observed (non symmetric peaks, shifting of individual resonance frequencies) especially for the measurement degrees of freedom on the crankshaft main bearing cap itself. The main cause of the nonlinearity is assumed in tilting induced friction in the flank contact regions.

To verify that the friction between the crankshaft main bearing cap and crank case is the cause for the nonlinearity, a second modal test was performed. Here, the flanks of the crankshaft main bearing cap were reduced to allow for clearance between the two parts. The test was performed in analogy to the first test, and 26 mode shapes could be identified in the investigated frequency range up to 4 kHz (one less). The quality of the identified data was very good in general. It was found that no more nonlinear behavior was present in the data. Furthermore the frequency of the tilting mode of the crankshaft main bearing cap is reduced significantly, indicating that friction induced stiffness is missing.

In order to classify the nonlinearity, and to obtain data for comparison with analytical data, step sine tests were performed. For these tests the excitation forces were controlled within a defined band around the target excitation force, and data was acquired for the configurations without and with friction between crankshaft main bearing cap and crank case. Figure 7 shows the test setup and figure 8 displays the measurement degrees of freedom on the crankshaft main bearing cap.

Figure 7: Test setup with modal exciter   Figure 8: Crankshaft main bearing cap

The basic principle of the step sine test is outlined in the following: At first the frequency band and the required frequency resolution are defined. If closed loop control is to be applied, a control channel is selected (here, the channel of the excitation force is taken for subsequent correlation with analytical data coming from harmonic balance calculations). The control itself is performed within a selected tolerance band around the ideal level (here, excitation force amplitude level), while the control is done within every single iteration step. The drawback of rather long measurement times is compensated by various advantages allowing for a dedicated analysis of the nonlinearity. Especially the defined excitation of the system at every frequency line, and the acquisition of data under steady state conditions (no transient effects) are to be named.

For the assembly the following frequency ranges were investigated. One holds a global mode of the system, the other one the local tilting mode of the crankshaft main bearing cap. Figure 9 and figure 10 show the measured spectra of the excitation force. It can be seen that the force level can be controlled very well.

1) Assembly with friction

1a) 1190 Hz … 1220 Hz (0.25 Hz resolution)	force amplitude	1,5 N $\pm$ 3%
		7,5 N $\pm$ 3%
		15,0 N $\pm$ 3%
1b) 1460 Hz … 1560 Hz (0.25 Hz resolution)	force amplitude	1,5 N $\pm$ 3%
		7,5 N $\pm$ 3%
		15,0 N $\pm$ 3%
		18,0 N $\pm$ 3%

2) Assembly without friction

2a) 1190 Hz … 1220 Hz (0.25 Hz resolution)	force amplitude	1,5 N $\pm$ 3%
		7,5 N $\pm$ 3%
		15,0 N $\pm$ 3%
2b) 1350 Hz … 1400 Hz (0.25 Hz resolution)	force amplitude	1,5 N $\pm$ 3%
		7,5 N $\pm$ 3%
		15,0 N $\pm$ 3%
		18,0 N $\pm$ 3%

Figure 9: Force spectra – with friction

Figure 10: Force spectra – without friction

Figures 11 to 14 below by example show the acceleration spectra at the top of crankshaft main bearing cap in normal (axial) direction. For the global mode (ranges 1a/2a) a weak damping nonlinearity can be observed. With increasing force amplitude level the damping increases. Also a slight decrease of stiffness is present.
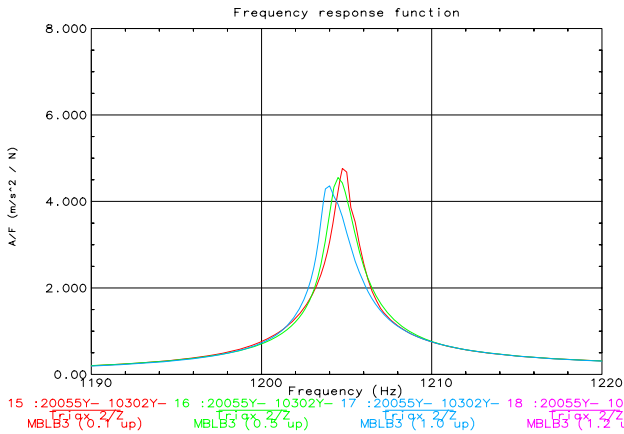

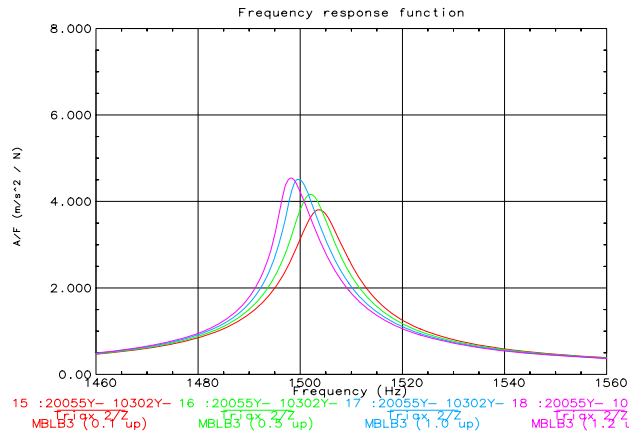Figure 11: Range 1a:
Acceleration spectra with friction

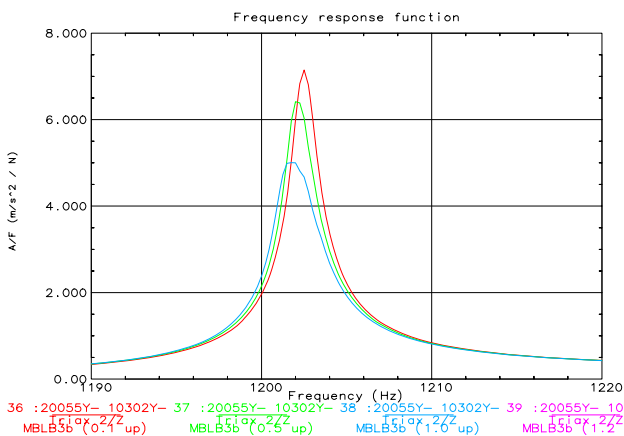Figure 12: Range 1b:
Acceleration spectra with friction

Figure 13: Range 2a:
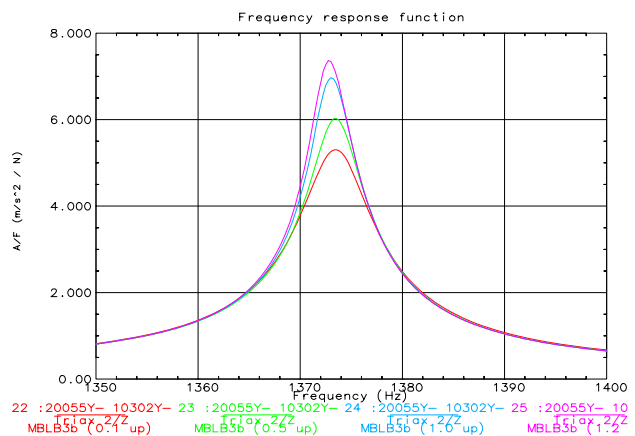Acceleration spectra without friction

Figure 14: Range 2b:
Acceleration spectra without friction

For the local mode (ranges 1b/2b) in general a damping nonlinearity can be observed. However, here the damping decreases with increasing force amplitude level. Also, the decrease of stiffness is present again. For the assembly with friction this effect can clearly be seen – the resonance frequency drops by about 5.5 Hz from the lowest to the highest force amplitude level (for the assembly without friction the drop is less than 1 Hz).

All in one the following conclusions can be drawn:

1) The resonance frequency increases for the assembly with friction by 2.5 Hz for the first range; for the second range the increase is about 125 to 130 Hz (depending on the force amplitude level). This indicates that the friction leads to a significant increase of stiffness for the tilting mode of the crankshaft main bearing cap.

2) The overall damping level is higher for the assembly with friction than for the assembly without friction.

Before modeling the flank contacts in order to account for the nonlinear friction effects, the bolt connection is investigated alone. This is accomplished by focusing on the data of the assembly without friction at first. Here, no (or negligible) additional friction effects are present. Table 3 shows the correlation results for the bolt connection model according to figure 5. The maximum frequency deviation of 6.51 Hz occurs for the tilting mode of the crankshaft main bearing cap. Obviously the selected modeling strategy is to stiff and needs to be revised.

State	Number of Test Modes Available	Number of Test Modes Paired	Mean Frequency Deviation [Hz]	Maximum Frequency Deviation [Hz]	Mean MAC Value [%]	Minimal MAC Value [%]
Initial	26	22	0.28	6.51	91.72	72.22

Table 3: Initial correlation for assembly without friction

Two alternative variants for the bolt connection were developed:

Variant 1 (Figure 15)

- connection of crankshaft main bearing cap to crank case via coincident nodes and rigid elements
- modeling of bolt as solid model
- connection of bolt via coincident nodes and rigid elements (RBE2)

Variant 2 (Figure 16)

- connection of crankshaft main bearing cap to crank case via coincident nodes and rigid elements
- modeling of bolt as lumped mass
- connection of bolt mass via constraint element (RBE3)
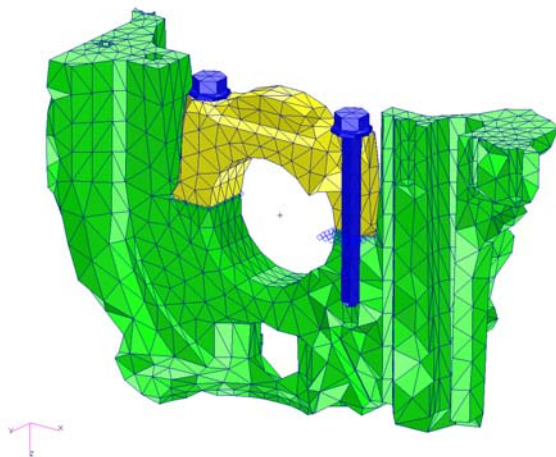

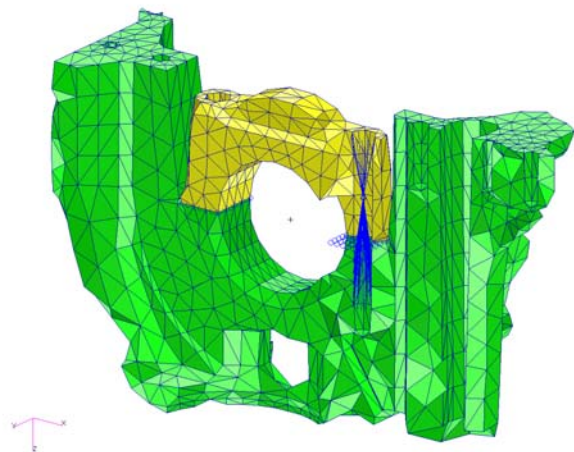Figure 15: Variant 1   Figure 16: Variant 2

Table 4 shows the correlation results for variants 1 and 2. For both variants excellent correlation results can be achieved. Especially for the tilting mode of the crankshaft main bearing cap, the frequency deviations are in both cases smaller than 2 %. Thus the two variants are equally suited for modeling the bolt connection.

State	Number of Test Modes Available	Number of Test Modes Paired	Mean Frequency Deviation [Hz]	Maximum Frequency Deviation [Hz]	Mean MAC Value [%]	Minimal MAC Value [%]
Variant 1	26	24	-0.29	-2.80	95.21	87.54
Variant 2	26	24	-0.36	-2.81	95.42	87.18

Table 4: Correlation for assembly without friction - variants

It was noted that test modes 19 and 20 could not be paired with MAC values greater than 70 % for either of the two variants. A closer look at these test modes shows that they are very closely spaced in the FE analysis (frequency deviation of about 3.6 % for corresponding analysis modes). A new correlation utilizing subspace pairing techniques (see also [6]), that allow for the correlation of linear combinations of mode shapes, finally yields a correlation of all 26 test modes. The MAC values of the formerly not paired modes increase to over 85 %, and the frequency deviations are less that 1 Hz.

After adequate modeling of the bolt connection, the friction at the flanks contacts shall now be taken into account. To accomplish this, the data from the step sine test are utilized. The analytical calculation of the corresponding frequency response functions is done in two different ways: one based on linearized calculation (harmonic balance), one based on a linear FE model.

For the first option, the calculation of the analytical frequency response functions is performed as outlined in section 2. Among others this allows for the direct analysis of different force levels. The analysis itself is conducted with the validated models of the components and the interface variant 2. For the second option, a linear FE model – also based on the validated FE models and interface variant 2 – is used. To account for the contact, linear springs are added in the contact area. The spring stiffnesses are set to values extracted from the linearized calculation using harmonic balance. Damping is introduced via individual modal damping of the mode shapes, and the different force levels can be accounted for by different spring stiffness and/or damping values. For practical applications, however, the selection of these parameters a priori may be difficult.

Figure 17 shows a comparison between test and analysis results for the excitation position for both investigated frequency ranges. In figures 18 and 19 the three normal (axial) measurement degrees of freedom on the crankshaft main bearing cap are presented. All in one a good agreement between test and analysis can be obtained. The linearized analysis, however, slightly overestimates the degree of nonlinearity. Both analysis options yet allow for the correct inclusion of the additional stiffness due to friction (second frequency range). Thus they are both equally suited for modeling the nonlinear stiffening effects in flank contact region.
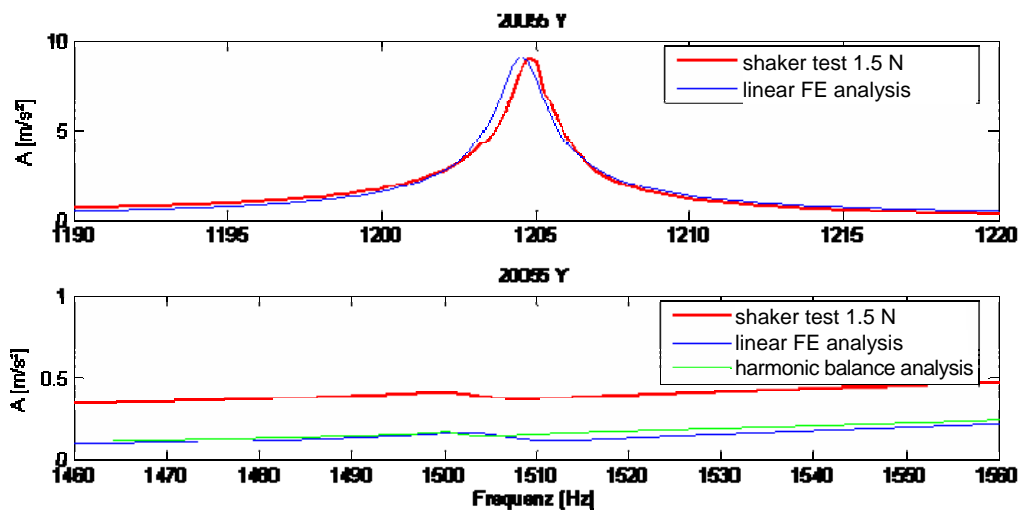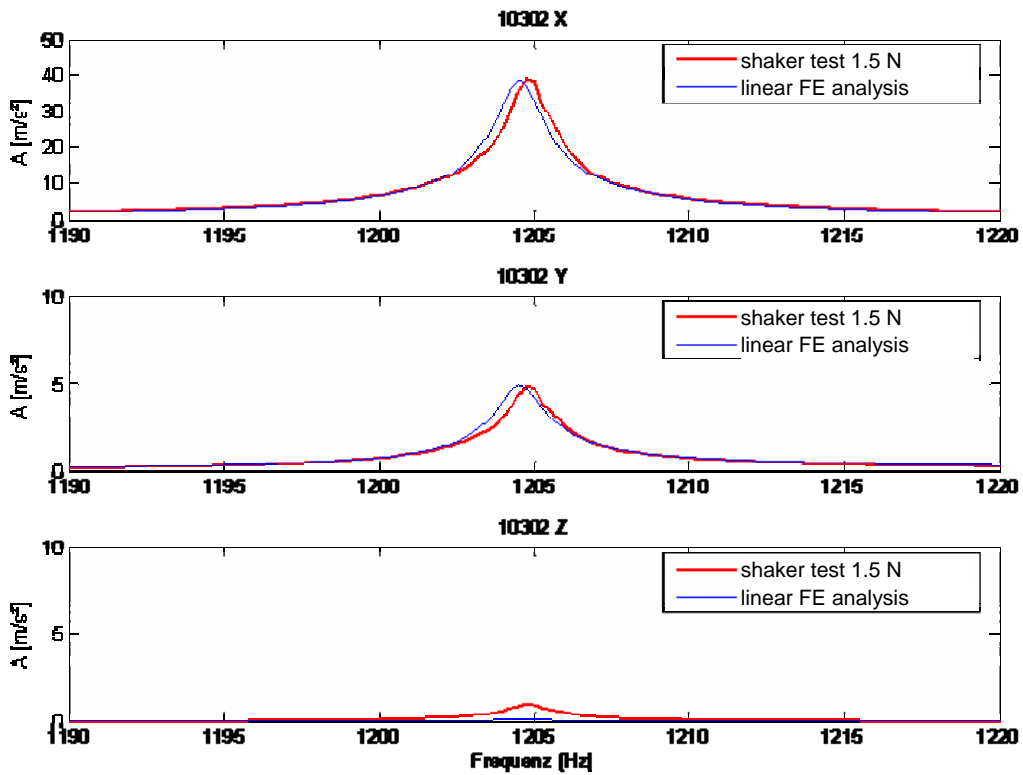

Figure 17: Frequency responses at excitation point

Figure 18: Frequency responses on crankshaft main bearing cap – frequency range 1
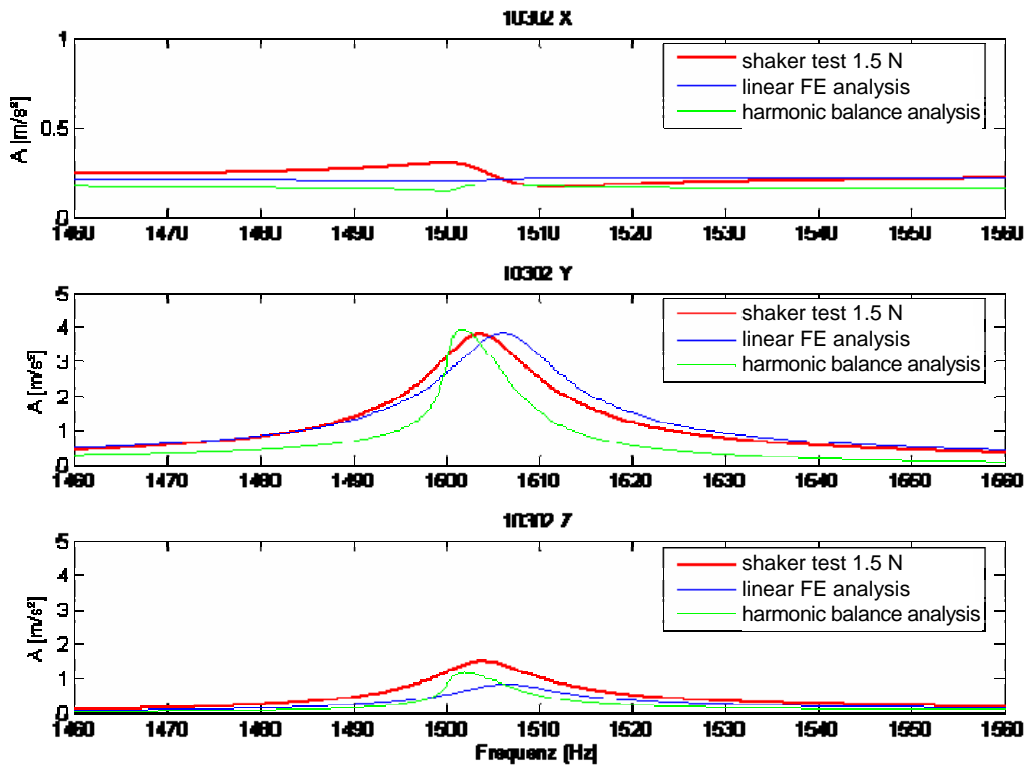

Figure 19: Frequency responses on crankshaft main bearing cap – frequency range 2

4   Summary

This paper highlighted the modeling of assembled combustion engine parts. Here multiple flange connections are found that contribute to the stiffness and damping characteristics. By example of a four cylinder combustion engine a FE modeling technique was introduced which focuses on a suitable and proper representation of the flange regions between crankcase and crankshaft main bearing cap.

The coupling of the crankcase and the main bearing cap consists of four interfaces, two bolt connections and two flank contacts. It could be shown, that the bolt connections can be modeled adequately using linear FE models. For the flank contacts, however, friction effects are present, that have to be accounted for.

To represent the friction at the flank contacts, two different approaches were applied. One is based on linear FE models with additional springs to capture the friction induced stiffness. The other is based on a special numerical procedure founded on the harmonic balance method, capable of modeling nonlinear damping and stiffness characteristics of the system.

Both approaches were compared to experimental data, and the effectiveness of the methods was shown. Especially, the numerical procedure based on the harmonic balance method is capable of directly forecasting the forced response of the system under different loading conditions. For the method based on linear FE models, the different loading conditions must be taken into account by adjusting spring stiffnesses and damping individually.

5   Acknowledgements

References

[1]   Link, Michael: *Updating of Analytical Models – Review of Numerical Procedures and Application Aspects*, Structural Dynamics Forum SD 2000, Los Alamos, New Mexico, USA (April 1999)

[2]   Schedlinski, Carsten, et al.: *Experimental Modal Analysis and Computational Model Updating of a Body in White*, Proceedings of the Noise and Vibration Engineering Conference, ISMA 2004, Leuven, Belgien, 2004

[3]   Sextro, Walter, *Dynamical Contact Problems with Friction:* Lecture Notes in Applied Mechanics Vol. 3, Berlin, Springer- Verlag (2002).

[4]   Popp, K., Panning, L., Sextro, W.: *Vibration Damping by Friction Forces: Theory and Applications*, Journal of Vibration and Control 9 (2003), pp.419- 448.

[5]   Johnson, K. L.: *Contact Mechanics*, Cambridge University Press, Cambridge, New York, Melbourne (1989), pp. 397- 423.

[6]   Schedlinski, Carsten, Staples, Bernard: *Computational Model Updating of Axisymmetric Systems*, Proceedings of the Noise and Vibration Engineering Conference, ISMA 2004, Leuven, Belgien, 2004